

RESEARCH

Open Access



The metabolic engineering of *Escherichia coli* for the high-yield production of hypoxanthine

Siyu Zhao^{1,2}, Tangen Shi^{1,2}, Liangwen Li^{1,2}, Zhichao Chen^{1,2}, Changgeng Li^{1,2}, Zichen Yu^{1,2}, Pengjie Sun^{1,2} and Qingyang Xu^{1,2*}

Abstract

Background Hypoxanthine, prevalent in animals and plants, is used in the production of food additives, nucleoside antiviral drugs, and disease diagnosis. Current biological fermentation methods synthesize quantities insufficient to meet industrial demands. Therefore, this study aimed to develop a strain capable of industrial-scale production of hypoxanthine.

Results De novo synthesis of hypoxanthine was achieved by blocking the hypoxanthine decomposition pathway, thus alleviating transcriptional repression and multiple feedback inhibition, and introducing a purine operon from *Bacillus subtilis* to construct a chassis strain. The effects of knocking out the IMP(Inosine 5'-monophosphate) branch on the growth status and titer of the strain were then investigated, and the effectiveness of adenosine deaminase and adenine deaminase was verified. Overexpressing these enzymes created a dual pathway for hypoxanthine synthesis, enhancing the metabolic flow of hypoxanthine synthesis and preventing auxotrophic strain formation. Introducing IMP-specific 5'-nucleotidase addressed the issue of adenylate accumulation. In addition, the metabolic flow of the guanine branch was dynamically regulated by the *guaB* gene. The supply of glutamine and aspartic acid precursors was enhanced by introducing an exogenous *glnA* mutant gene, overexpressing *aspC*, and replacing the weaker promoter to regulate the aspartic acid branching pathway. Ultimately, fermentation in a 5 L bioreactor for 48 h produced 30.6 g/L hypoxanthine, with a maximum real-time productivity of 1.4 g/L/h, the highest value of hypoxanthine production by microbial fermentation reported so far.

Conclusions The intracellular purine biosynthesis pathway is extensive and regulated at multiple levels in cells. The IMP branch in the hypoxanthine synthesis pathway has a higher metabolic flux. The current challenge lies in systematically allocating the metabolic flux within the branch pathway to achieve substantial product accumulation. In this study, *E. coli* was used as the chassis strain to construct a dual pathway for IMP and AMP(Adenosine 5'-monophosphate) synergistic hypoxanthine synthesis and dynamically regulate the guanine branch pathway. Overall, our experimental efforts culminated in a high-yield, plasmid- and defect-free engineered hypoxanthine strain.

Keywords Hypoxanthine, Dual pathway, De novo synthesis, *Escherichia coli*, Metabolic engineering, Dynamic regulation

*Correspondence:

Qingyang Xu
xqingyang@tust.edu.cn

¹College of Biotechnology, Tianjin University of Science & Technology, Tianjin 300457, P. R. China

²Key Laboratory of Industrial Fermentation Microbiology, Ministry of Education, Tianjin University of Science & Technology, Tianjin 300457, P. R. China



© The Author(s) 2024. **Open Access** This article is licensed under a Creative Commons Attribution-NonCommercial-NoDerivatives 4.0 International License, which permits any non-commercial use, sharing, distribution and reproduction in any medium or format, as long as you give appropriate credit to the original author(s) and the source, provide a link to the Creative Commons licence, and indicate if you modified the licensed material. You do not have permission under this licence to share adapted material derived from this article or parts of it. The images or other third party material in this article are included in the article's Creative Commons licence, unless indicated otherwise in a credit line to the material. If material is not included in the article's Creative Commons licence and your intended use is not permitted by statutory regulation or exceeds the permitted use, you will need to obtain permission directly from the copyright holder. To view a copy of this licence, visit <http://creativecommons.org/licenses/by-nc-nd/4.0/>.

Background

Hypoxanthine is a highly important biological substance, participating in the regulation of some important physiological functions in the human body [1] and exhibiting pharmacological activities such as lowering blood pressure, relieving asthma, and treating gout. In medicine, hypoxanthine and its derivatives are used to produce nucleoside antiviral drugs and immunosuppressants [2]. In industrial production, hypoxanthine is a precursor for various chemical products like mercaptopurine and azathioprine [3]. In agriculture, hypoxanthine acts as a bactericide and pesticide intermediate, highlighting its economic and social value.

Currently, hypoxanthine is primarily produced in industry through the hydrolysis of inosine. However, this process faces several challenges, including high production costs, significant environmental impact, and complex extraction procedures. In contrast, microbial fermentation offers an efficient, cost-effective, and sustainable alternative, which has already been successfully applied to large-scale production of various natural compounds [4, 5]. *Escherichia coli* is considered a promising strain for purine nucleotide production due to its excellent availability in molecular biology and genomic tools [6]. Previously, the biological synthesis of hypoxanthine in *E. coli* was achieved for the first time [7], providing a reference for constructing subsequent strains. However, this approach still results in hypoxanthine yields at the milligram level, indicating considerable potential for improvement.

Purine biosynthesis in *E. coli* is a tightly regulated process essential for maintaining cell homeostasis and energy supply [8–10]. To overcome limitations in this pathway, Min Liu et al. [7] addressed the branch involving the key precursor inosine 5'-monophosphate (IMP) and the pentose phosphate pathway. They achieved this by relieving purine feedback inhibition, removing transcriptional repression, and knocking out the global regulatory factor *arcA*. Their approach led to the production of 1243 mg/L hypoxanthine through fed-batch fermentation. Ting Shi et al. [4] enhanced riboflavin production by improving purine nucleotide supply, disrupting the 5'-UTR of the PurR repressor protein and the guanine-sensitive ribose switch in the purine operon. They also upregulated the transcription of purine genes by approximately 380 times. SHIMAOKA et al. [11] overexpressed the mutant genes *purE*^{K326Q,P410W} and *prs*^{D128A} in *Escherichia coli* I-9 m, alleviating feedback inhibition of rate-limiting enzymes and increasing inosine production by 3.6-fold. Previous studies [12] have demonstrated that the repressor protein PurR regulates target genes by binding to small molecules like hypoxanthine or guanine [13]. Therefore, knocking out PurR is necessary for overcoming this regulation.

Initially, we engineered a chassis strain by blocking the decomposition pathway, alleviating feedback inhibition, and introducing exogenous purine operons. We then validated the effectiveness of adenosine deaminase and adenine deaminase, using them to create a dual pathway for the synergistic synthesis of hypoxanthine from IMP and adenosine 5'-monophosphate (AMP), resulting in a non-adenine auxotrophic strain. We also introduced exogenous IMP-specific nucleases to address adenosine monophosphate accumulation and knocked out the hypoxanthine to inosine pathway to facilitate replenishment. Additionally, we incorporated the *Bacillus subtilis* mutants *glnA*_{bsu}^{L159I, E304A}, which overexpress the *aspC* gene encoding aspartate synthase. We optimized the main pathway by adjusting the promoters of the aspartic kinase *thrA* gene to find the ideal intensity for maximizing both yield and conversion rate. After 48 h of fermentation in a 5 L fermenter, hypoxanthine production reached 30.6 g/L, with a maximum real-time yield of 1.4 g/L/h, and minimal by-product accumulation. The metabolic pathway diagram of hypoxanthine is shown in Fig. 1.

Materials and methods

Chemical reagents

Glucose monohydrate was purchased from Pengyuan Starch Co., Ltd. in Qinhuangdao, China, and yeast powder was purchased from Lesaff Management (Shanghai) Co., Ltd. DNA polymerase was purchased from Nanjing Novozan Biotechnology Co., Ltd. In addition, oligonucleotide primers (Supplementary Table 1) were synthesized by Tianjin Jinweizhi Biotechnology Co., Ltd. All other analytical grade reagents were purchased from Aladdin Biochemical Technology Co., Ltd. in Shanghai, China.

Plasmids, strains, and culture conditions

The plasmids and engineering strains used in this study are listed in Table 1. *Escherichia coli* DH5 α was used for the construction and cloning of plasmid vectors, whereas molecular modification was conducted based on *Escherichia coli* W3110. Plasmids, namely, pREDCas9 and pGRB, were used as part of a CRISPR/Cas9 gene editing system [14]. If necessary, add 100 mg/L of ampicillin, 50 mg/L of spectinomycin, 0.2 mM of isopropyl β -D-thiogalactoside (IPTG), and 0.2% (w/v) of L-arabinose.

Acquisition of target genes

The endogenous target genes used in this study were amplified using the genomic DNA of *Escherichia coli* W3110 as a template, whereas the heterologous genes were artificially synthesized (Jin Weizhi, Tianjin) and optimized via the application of codons. Specifically, the acquisition of the target gene *add* is based on the *Escherichia coli* W3110 genome as a template, and s/a

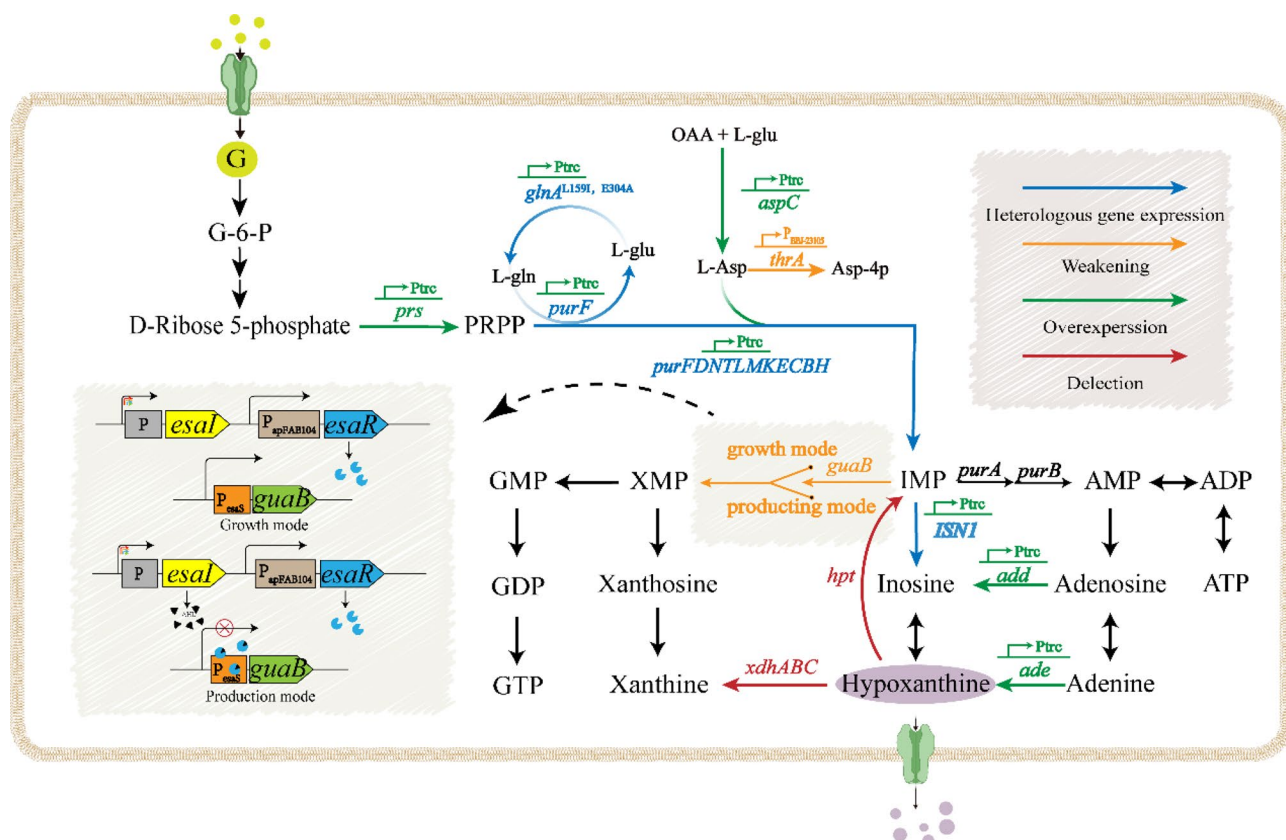


Fig. 1 Metabolic pathway diagram of hypoxanthine. The blue arrow represents the introduction of heterologous genes, the yellow arrow represents the weakening gene, the green arrow represents the overexpressed gene, and the red arrow represents the deletion of related genes. *purF*, *glnA*, and *pur* (*FDNTSQLMKECB*) were from *Bacillus subtilis*, and *isn1* were from *Saccharomyces cerevisiae*

amplification was performed using primers. The *ISN1* gene derived from brewing yeast is obtained by optimizing codons, synthesizing plasmids as templates, and amplifying s/a with primers.

Genome editing

The strain was modified by CRISPR / Cas9 gene editing system [15]. Here, the deletion of the *xdhABC* gene is used as an example. Firstly, the pGRB-*xdhABC* plasmid was constructed, and the 20 bp spacer sequence was screened by CRISPR RGEN Tools (<http://www.rgenome.net/>). Then the complementary primers (gRNA-*xdhABC*-1 and gRNA-*xdhABC*-2) were synthesized and annealed to form dsDNA, which contained the spacer sequence and flanking sequence homologous to the pGRB skeleton. The dsDNA was ligated with the linearized pGRB plasmid. The two homologous arms of *xdhABC* were amplified by primers *xdhABC*-U1 / *xdhABC*-U2 and *xdhABC*-D1 / *xdhABC*-D2, and DNA-*xdhABC* was obtained by overlapping polymerase chain reaction. DNA-*xdhABC* and pGRB-*xdhABC* were co-transformed into pRED-Cas9. To integrate the target gene into the chromosome, two homologous arms are

linked to the gene to form the donor DNA. The remaining steps follow the previously described procedure.

Shake flask fermentation cultivation

Take 10ul of bacterial solution from a glycerol tube and transfer it to a shaking tube containing LB medium. Incubate at 37 °C, 225 rpm, and activate for 15 h. Next, take 2mL of the activated bacterial solution and inoculate it into a 500mL shaking flask containing 30mL of fermentation medium. Cultivate the flask at 37 °C and 225 rpm for 26 h. The fermentation medium contained: 30 g/L glucose, 2.5 g/L citric acid monohydrate, 10 mg/L $\text{MnSO}_4 \cdot \text{H}_2\text{O}$, 4.5 g/L KH_2PO_4 , 2 g/L $(\text{NH}_4)_2\text{SO}_4$, 2 g/L $\text{MgSO}_4 \cdot 7\text{H}_2\text{O}$, 40 mg/L $\text{FeSO}_4 \cdot 7\text{H}_2\text{O}$, 5 g/L yeast extract, 2 g/L peptone, 2 mg/L V_{H} , 2 mg/L $\text{V}_{\text{B1,3,5,12}}$, 8 mg/L phenol red (pH 7.0–7.2). During fermentation, adjust the pH of the broth to approximately 6.7 by adding 25% (v/v) ammonium hydroxide, based on the observed color change in the broth.

Fed-batch fermentation in a 5-L bioreactor

Begin by preparing 2 L of seed culture medium in a 5 L bioreactor. Use an LB shaker to wash the bacterial cells from the inclined surface of the medium and transfer

Table 1 Strains and plasmids used in this study

Strains	Characteristics	Source
<i>E. coli</i> DH5α	Host for cloning	Lab stock
<i>E. coli</i> W3110	Wild type, starting strain	Lab stock
HX1	<i>E. coli</i> W3110, $\Delta xdhABC$	This study
HX2	HX1, $\Delta purR$	This study
HX3-1	HX2, $ygay::P_{trc}-purF_{eco}^{K326QP410W}$	This study
HX3-2	HX2, $ygay::P_{trc}-purF_{bsu}^{D293V,K316Q,S400W}$	This study
HX4-1	HX3-2, $yeeep::P_{trc}-prs_{baz}^{N120S,L135I}$	This study
HX4-2	HX3-2, $yeeep::P_{trc}-prs_{eco}^{D128A}$	This study
HX5	HX4-2, $ilvg::P_{trc}-pur$ (FDNTSQLMKECB)	This study
HX1-1	HX5, $\Delta purA$	This study
Y1-2	HX5, $purA_{bsu}^{P242N}$	This study
Y2-1	HX5, Δadd	This study
Y2-2	HX5, $ycgh::add(eco)$	This study
Y2-3	HX5, $ycgh::add(sce)$	This study
Y2-4	HX5, $ycgh::add(stm)$	This study
Y3-1	HX5, Δade	This study
Y3-2	HX5, $yjit::P_{trc}-ade(eco)$	This study
Y3-3	HX5, $yjit::P_{trc}-ade(sce)$	This study
Y3-4	HX5, $ycgh::P_{trc}-add(eco)$, $yjit::P_{trc}-ade(eco)$	This study
Y4-1	Y3-4, $mbhA::P_{trc}-ushA$, $gapC::P_{trc}-nagD$, $arpB::P_{trc}-surE$	This study
Y4-2	Y3-4, $ylbe::P_{trc}-isn1(sce)$	This study
Y4-3	Y4-2, Δhpt	This study
Y5-1	Y4-3, $\Delta guaB$	This study
Y5-2	Y4-3, $rph::P_{apFAB104}-EsaR$	This study
Y5-3	Y5-2, $yghe::P_{esa5}-guaB$	This study
A	Y5-3, $ycdn::P_{Bba_j23114}-esal$	This study
B	Y5-3, $ycdn::P_{Bba_j23110}-esal$	This study
C	Y5-3, $ycdn::P_{Bba_j23101}-esal$	This study
D	Y5-3, $ycdn::P_{Bba_j23100}-esal$	This study
Y6	HX5-3, $yjip::P_{trc}-pur$ (FDNTSQLMKECB)	This study
Y6-1	Y6, $yeeL::P_{trc}-glnA_{bsu}^{L159I,E304A}$	This study
Y6-2	Y6-1, $yjgx::P_{lac}-aspC$	This study
Y6-3	Y6-2, $\Delta thrA$	This study
Y6-4	Y6-2, $ynci::P_{Bba_j23109}-thrA$	This study
Y6-5	Y6-2, $ynci::P_{Bba_j23114}-thrA$	This study
Y6-6	Y6-2, $ynci::P_{Bba_j23105}-thrA$	This study
Y6-7	Y6-2, $ynci::P_{Bba_j23110}-thrA$	This study
pRed-cas9	Cas9 expression vector	Lab stock[14]
pGRB	gRNA expression vector	Lab stock[14]

them to a fermentation tank for seed cultivation. The same medium used for shake flask cultures is employed here, except phenol red is omitted. Once the culture reaches an OD600 of 20, retain 400mL of bacterial liquid and use a peristaltic pump to add fresh fermentation medium, bringing the volume back to 2 L. The system automatically adds ammonium hydroxide to maintain the pH at approximately 6.7, while temperature is controlled at 37 °C. Stirring speed and aeration rate are adjusted to keep the dissolved oxygen above 50%. Samples are

collected every two hours to monitor the remaining glucose levels, and the sugar replenishment rate is adjusted as needed to maintain glucose in a suboptimal range.

Analytical methods

Spectrophotometer (SR-2800PC, Shanghai Sheyan Instrument Co., Ltd.) to detect the cell growth status. Glucose concentration was measured by glucose analyzer (HG06-SBA-50, Beijing Beixin Chuangzhan Automation Technology Co., Ltd.). High performance liquid chromatography (LC-100, Shanghai Wufeng Scientific, Shanghai, China) was used to quantify the standard of hypoxanthine, and the sample was quantified at the wavelength of 260 nm; a 250 mm×4.6 mm, 5 μm column was used with a column temperature of 30 °C; and 5% acetonitrile phosphate solution was used as the mobile phase with a flow rate of 1 mL/min. Prepare standard curves using diluted hypoxanthine solutions at concentrations of 0.01 g/L, 0.05 g/L, and 0.1 g/L. Collect samples every two hours to monitor changes in hypoxanthine production.

Statistical analysis

Data represent the mean and standard deviation of three independent experiments. One-way analysis of variance and Dunnett's multiple comparison tests determined significant differences between data. A P-value (0.01 < P < 0.05) indicated significant differences, while P < 0.01 indicated very significant differences.

Results

Constructing the hypoxanthine chassis strain

Conventional metabolic engineering methods were employed. Initially, the hypoxanthine decomposition pathway was disrupted by knocking out the *xdhABC* gene in wild-type *E. coli* W3110, preventing the decomposition of hypoxanthine to xanthine. This yielded strain HY1, which produced 50 mg/L hypoxanthine after 24 h shake-flask fermentation. The *lacI* gene was deleted in strain HY1 to ensure the constitutive expression of genes controlled by the P_{trc} promoter. The purine repressor (PurR) has been shown to bind to the operon sequence, subsequently having a negative impact on pur operon gene expression [12]. The binding of PurR to hypoxanthine, adenine, or guanine [16] changes its conformation [17], thereby hindering purine nucleotide biosynthesis. Therefore, the *purR* gene was knocked out, creating strain HY2 (Fig. 2). This process culminated in the accumulation of 0.1 g/L of hypoxanthine after 24 h fermentation, consistent with previous studies.

In *E. coli*, amidophosphoribosyltransferase (encoded by the *purF* gene) is a key rate-limiting enzyme in the de novo synthesis of purine nucleosides. *purF* catalyzes the production of 5-phosphate ribosamine and glutamic acid from PRPP and glutamine, but its catalytic activity

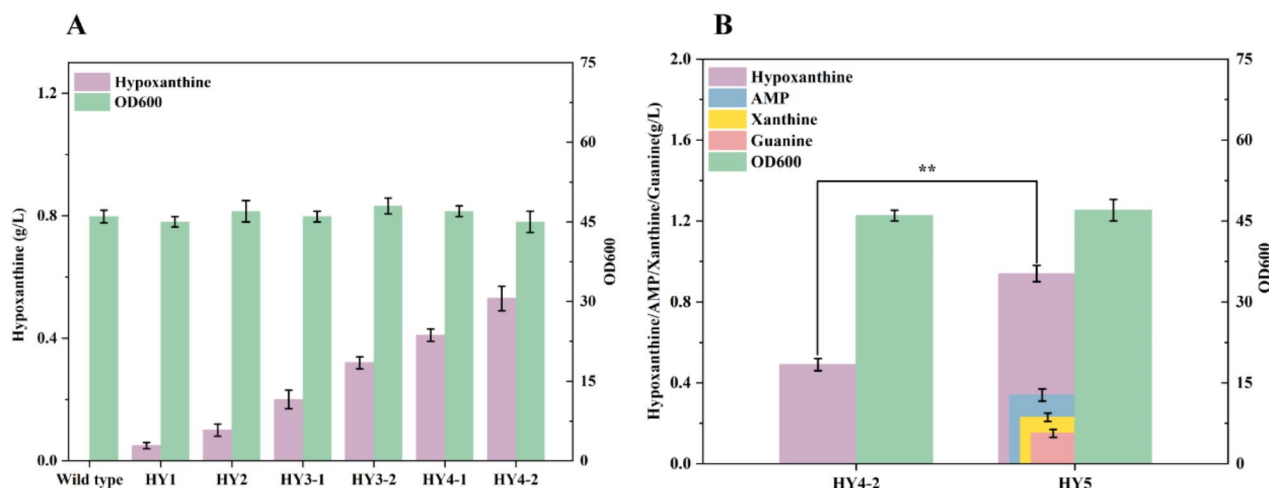


Fig. 2 (A) Shake-flask fermentation data of chassis strain process bacteria. (B) Effect of *Bacillus subtilis* purine operon on strain HY5. Shake-flask data are expressed as means, and the error bars represent the standard deviation ($n=3$ independent experiments)

is inhibited by the synergistic feedback of AMP and Guanosine 5' -phosphate (GMP) [11]. The *purF* genes in *E. coli* and *B. subtilis* can relieve feedback inhibition via site-directed mutagenesis [4]. In this study, mutant genes *purF*_{eco}^{K326Q, P410W} and *purF*_{bsu}^{D293V, K316Q, S400W} were integrated into the *ygay* pseudogene locus of HY2 and controlled by the P_{trc} promoter to construct strains HY3-1 and HY3-2 respectively. As shown in Fig. 2, the hypoxanthine titer of HY3-1 was 0.2 g/L, while the hypoxanthine titer of HY3-2 was higher (0.32 g/L), indicating that the *purF*_{bsu}^{D293V, K316Q, S400W} mutation was more effective.

PRPP is catalyzed by phosphoribosylpyrophosphate synthase (encoded by the *prs* gene), but its catalytic activity is inhibited by feedback from Adenosine-5' -diphosphate and Guanosine-5' -diphosphate. The introduction of D128A mutation in *prs* of *E. coli* [11] and N120S and L135I mutations in *prs* of *B. amyloliquefaciens* [18] can relieve this inhibition of PRPP synthase, thereby enhancing the reaction. We constructed *prs*_{baz}^{N120S, L135I}, and *prs*_{eco}^{D128A} on the *yeep* pseudogene locus of HY3-2, creating two PRPP synthase mutant gene strains, HY4-1 and HY4-2 (Fig. 2). Shake-flask fermentation results showed hypoxanthine titers of 0.41 g/L and 0.53 g/L for HY4-1 and HY4-2, respectively, demonstrating that *prs*_{eco}^{D128A} was more effective in enhancing hypoxanthine yields.

IMP is an important precursor to the synthesis purines such as hypoxanthine. Specifically, PRPP undergoes a ten-step enzymatic reaction to generate IMP, involving 12 genes (*purFDNTSQLMKECB*) that control the de novo synthesis pathway of purine nucleosides, which are scattered across different locations on the *E. coli* chromosome. However, in *B. subtilis*, the purine operon consists of three overlapping gene clusters [*purEKB-purCSQLF-purMNH* (*J*)] and a 3' -terminal *purD* gene [19, 20]. *B.*

subtilis has often been used for producing nucleoside compounds. To strengthen the purine synthesis pathway, the purine operon (*purEKBSQLGMNHD*) from *B. subtilis* was integrated into the *ilvG* pseudogene site of strain HY4-2, and strain HY5 was obtained by controlling the P_{trc} promoter. Shake-flask fermentation results showed a hypoxanthine titer of 0.94 g/L for HY5, with trace titers of adenine, xanthine, and guanine at 0.34 g/L, 0.23 g/L, and 0.15 g/L, respectively. The heterologous operon introduced in this study was efficiently expressed in *E. coli* W3110 without affecting bacterial growth.

Constructing a dual pathway for the synergistic synthesis of hypoxanthine by IMP and AMP

IMP is the first compound in the purine synthesis pathway with a complete purine ring. IMP has two branched pathways catalyzed by adenylosuccinate synthetase (encoded by *purA*) and IMP dehydrogenase (encoded by *guaB*) to produce adenine and guanine, respectively. Researchers have analyzed the metabolic flux of the IMP branch and found that the carbon metabolic flux towards the adenine branch greatly exceeds that towards the hypoxanthine and guanine branches [21], limiting hypoxanthine synthesis.

Dealing with the metabolic flux of the adenine synthesis pathway is crucial for improving hypoxanthine yield. First, we knocked out the adenosine succinate synthase-encoding gene *purA* to block the adenine branch, creating strain Y1-1 from strain HY5. The shake-flask fermentation results shown in Fig. 3B indicated a decrease in the OD600 value of strain Y1-1 to 31 and a hypoxanthine titer reduction to 0.49 g/L, with no accumulation of AMP, xanthine, or guanine. This indicates that the blockage of the adenine branch limits the synthesis of energy,

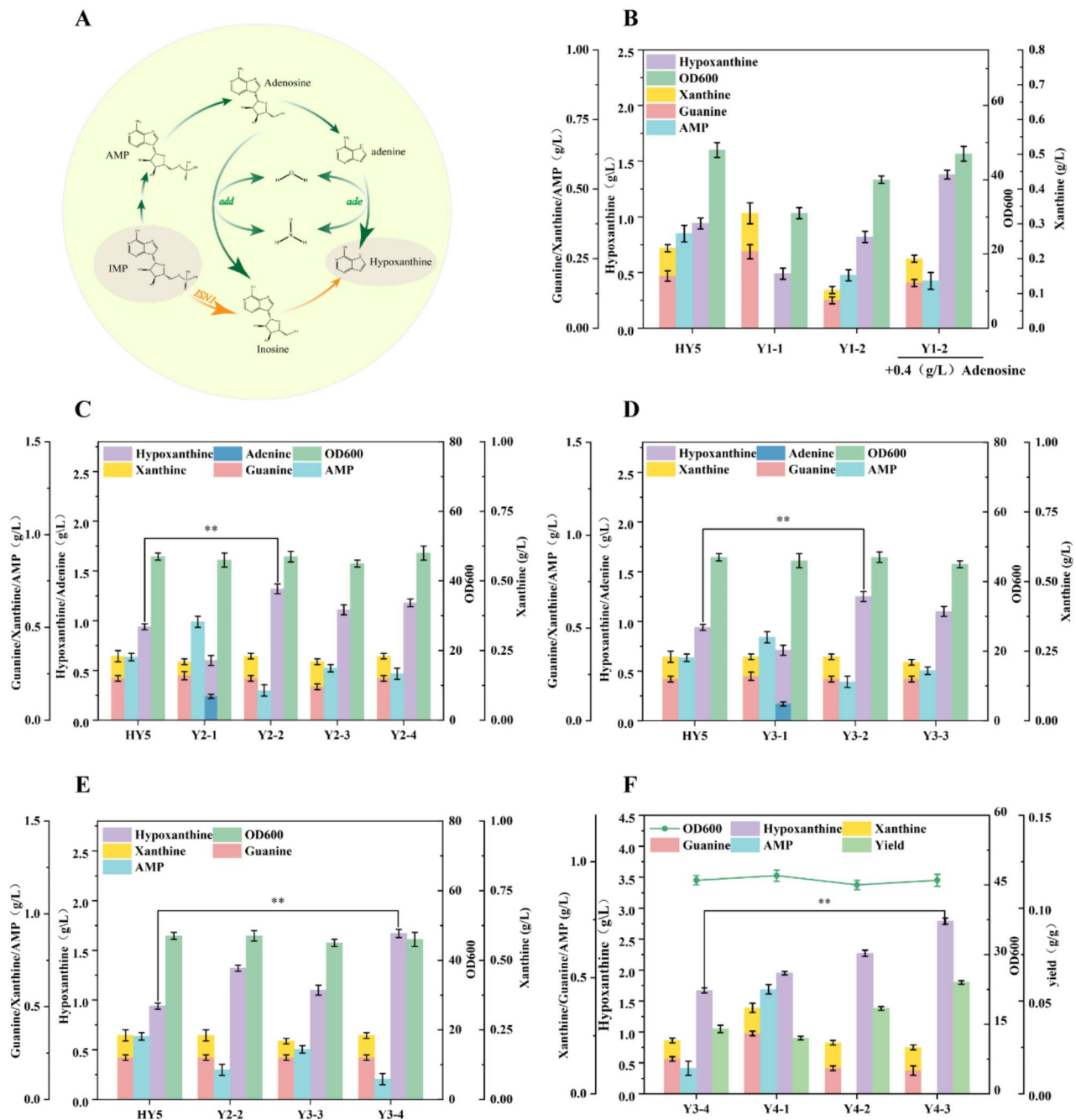


Fig. 3 (A) Schematic diagram of dual pathways for hypoxanthine synthesis. (B) Data on the effect of knockout and weakening of the *purA* gene on strains. (C) Effects of knockout or overexpression of adenosine deaminase on strains. (D) Effects of knockout or overexpression of adenine deaminase on strains. (E) Comparison of single and double overexpression of adenosine deaminase and adenine deaminase. (F) Overexpression of 5'- nucleotidase, and the impact of deleting hypoxanthine phosphoribosyltransfer (*hpt*) on bacterial strains. Data are expressed as means, and the error bars represent the standard deviation ($n=3$ independent experiments)

or nutrients required by the cell, which in turn adversely affects the growth and production of the cell, and this is not the result we want to see.

Recognizing the detrimental effects of directly blocking the adenine branch, we opted to weaken it instead. Studies have shown that substituting proline at position 242

of *purA* with asparagine in *B. subtilis* can reduce enzyme activity by 53.7% [22]. Using this approach, we replaced the *purA* gene of HY5 with the *purA*_{bsu}^{P242N} mutant gene to construct strain Y1-2. As shown in Fig. 3B, the hypoxanthine titer of Y1-2 was 0.82 g/L, with an OD600 value of 40 and an AMP accumulation of 0.19 g/L. Although

strain growth improved compared to the direct knockout, it did not fully recover. Adding 0.4 g/L adenosine increased the hypoxanthine titer of Y1-2 to 1.38 g/L, and the OD600 value normalized to 47. This demonstrated that the introduction of weaker adenosine succinate synthase restored strain growth and enhanced hypoxanthine titer more effectively than a direct knockout; however, the biomass and titer were further improved under these conditions. The results showed that even after using the strategy of weakening the adenine branch, the adenosine succinate synthase of this intensity has an effect; however, it still cannot produce high-yield hypoxanthine under the condition of satisfying the normal growth of the bacteria, prompting the search for a new solution to produce a high-yield strain that can be industrialized.

Adenosine deaminase, known for its high biocatalytic ability, completes its catalytic activity through a single polypeptide chain, in the absence of cofactors [23, 24]. Zengyi Chang et al. identified adenosine deaminase activity in cell extracts of *E. coli* via zymography [25]. This enzyme has been shown to catalyze the conversion of adenosine to inosine in *E. coli* and *Salmonella typhimurium* [26–28], pointing to induction of a higher metabolic flux into the hypoxanthine synthesis pathway, without weakening the adenine synthesis pathway. Overall, this outcome results in a dual pathway for hypoxanthine synthesis.

To verify adenosine deaminase activity in *E. coli*, we knocked out the adenosine deaminase-coding gene *add* in strain HY5, resulting in strain Y2-1, which is similar to strain HY5. Shake-flask fermentation for 24 h revealed a hypoxanthine titer decrease to 0.6 g/L, with adenylylate, xanthine, guanine, and adenine having increased to 0.53 g/L, 0.21 g/L, 0.16 g/L, and 0.24 g/L (Fig. 3C), respectively. This confirmed that adenosine deaminase activity in *E. coli* redirected more metabolic flux toward the hypoxanthine synthesis pathway. To determine if the introduction of exogenous adenosine deaminase could further enhance hypoxanthine accumulation, we integrated the adenosine deaminase-encoding gene *add* from *E. coli*, *S. cerevisiae*, and *S. typhimurium* into the *ycgh* pseudogene site of HY5, optimized the codon to obtain strains Y2-2, Y2-3, and Y2-4, and compared them with strain HY5. Shake-flask fermentation results showed (Fig. 3C) that strain Y2-2 accumulated 1.32 g/L hypoxanthine, 0.16 g/L adenine, 0.23 g/L xanthine, and 0.15 g/L guanine. Strain Y2-3 accumulated 1.11 g/L hypoxanthine, 0.28 g/L adenine, 0.23 g/L xanthine and 0.15 g/L guanine, respectively. Strain Y2-4 accumulated 1.18 g/L hypoxanthine, 0.25 g/L adenylylate, 0.23 g/L xanthine and 0.15 g/L guanine.

Compared with the strain HY5, the results showed that the adenosine deaminase from *E. coli*, *S. cerevisiae*, and *S. typhimurium* had varying degrees of positive effects on

hypoxanthine accumulation, with adenosine deaminase from *E. coli* having the most significant effect in promoting hypoxanthine synthesis. Overall, by overexpressing the adenosine deaminase *add* gene from *E. coli*, we successfully constructed an adenosine-inosine-hypoxanthine synthesis pathway (Fig. 3A).

In *S. cerevisiae*, adenine can be deaminated to hypoxanthine by adenine deaminase [29, 30]. Therefore, we hypothesized that in *E. coli*, adenine could similarly be converted to hypoxanthine via adenine deaminase. To test this, we conducted experiments on *E. coli*. We knocked out the adenine deaminase gene *ade* in strain HY5, creating strain Y3-1. Shake-flask fermentation results (Fig. 3D) showed that hypoxanthine titer decreased to 0.71 g/L, and adenylylate accumulation increased from 0.34 g/L to 0.45 g/L, while xanthine and guanine levels remained unchanged. These results indicate that knocking out adenine deaminase increased adenine accumulation to 0.17 g/L while reducing hypoxanthine production, confirming that adenine deaminase in *E. coli* effectively catalyzes the conversion of adenine to hypoxanthine. To explore whether exogenous adenosine deaminase plays a better role in *E. coli*, we overexpressed the adenine deaminase-encoding gene *ade* of *E. coli* and the codon-optimized adenine deaminase-encoding gene *aah1* of *S. cerevisiae* on the *yjit* pseudogene site of strain HY5, resulting in strains Y3-2 and Y3-3, respectively. Shake-flask fermentation (Fig. 3D) showed that hypoxanthine accumulation of strain Y3-2 was 1.25 g/L, and the adenylylate, xanthine, and guanine accumulations were 0.21, 0.23, and 0.15 g/L, respectively. The accumulation of hypoxanthine in strain Y3-3 was 1.1 g/L, with adenylylate, xanthine, and guanine at 0.27, 0.21, and 0.15 g/L, respectively. These findings show that both sources of adenosine deaminase promote hypoxanthine synthesis, although the exogenously introduced adenine deaminase was not as effective as the adenine deaminase from *E. coli*.

We then verified whether the simultaneous overexpression of adenosine deaminase and adenine deaminase has a synergistic effect. Overexpressing both the adenosine deaminase-encoding gene *add*, and the adenine deaminase-encoding gene *ade* from *E. coli* in strain HY5 resulted in strain Y3-4. Shake-flask fermentation (Fig. 3E) showed that the hypoxanthine titer increased to 1.67 g/L, a 77.66% increase compared to strain HY5, while adenylylate accumulation decreased to 0.11 g/L. No significant changes were observed in the accumulation of xanthine and guanine. These findings confirm that the simultaneous overexpression of adenosine deaminase and adenine deaminase synergistically enhanced hypoxanthine synthesis. At this point, we constructed a dual pathway for the synergistic synthesis of hypoxanthine by IMP and AMP, which effectively improved hypoxanthine titer;

however, the accumulation of adenylate, a by-product of the adenine branch, remains unclear.

The adenine synthesis pathway is strictly regulated by feedback inhibition [31]. After a thorough analysis of the adenine feedback inhibition mechanism, we replaced the purine operon gene cluster. However, the current accumulation of adenylate still causes feedback inhibition, which hinders the entire purine metabolic synthesis pathway. 5'-nucleotidase is an enzyme that catalyzes the production of nucleosides and phosphates from nucleoside monophosphates. To reduce the accumulation of intermediate adenylates, we overexpressed the *ushA*, *nagD*, and *surE* genes encoding 5'-nucleotidase on strain Y3-4, creating strain Y4-1. Shake-flask fermentation results (Fig. 3F) showed that hypoxanthine titer was 1.95 g/L, with no adenylate accumulation, and the accumulation of xanthine and guanine increased to 0.37 g/L and 0.26 g/L, respectively. The glycoside conversion rate decreased from 0.035 to 0.03 g / g. Generally, 5'-nucleotidase acts on AMP to produce adenosine, IMP to synthesize inosine, XMP (xanthosine 5-monophosphate) to synthesize flavin, and GMP to synthesize guanosine. It contributes to hypoxanthine accumulation and promotes by-product formation, resulting in a decrease in conversion rate. The gene *isn1* from *S. cerevisiae* encodes IMP-specific 5'-nucleotidase, which can specifically catalyze the decomposition of IMP into inosine [32]. Therefore, we introduced the IMP-specific 5'-nucleotidase to compete for more metabolic flux to the hypoxanthine synthesis pathway, reduce adenylate accumulation, and improve the conversion rate of product synthesis. A codon-optimized *isn1* gene controlled by the P_{trc} promoter was integrated into the *ylbe* pseudogene site of strain Y3-4 to generate strain Y4-2.

Interestingly, the heterologous introduction of 5'-nucleotidase *isn1* significantly enhanced hypoxanthine production. Compared to Y4-1, the hypoxanthine titer (2.27 g/L) of Y4-2 increased by 16.5% (Fig. 3F), and the glycoside conversion rate also significantly increased from 0.03 g/g to 0.046 g/g. The fermentation broth test results showed no adenylate accumulation, and strain growth remained normal. The above results showed that the expression of specific 5'-nucleotidase *isn1* gene improved IMP to inosine conversion, enhancing the reaction of IMP decomposition into inosine. The direction of hypoxanthine synthesis competed for more IMP metabolic flow without affecting the growth of the strain itself while resolving intermediate product adenylate accumulation issues and improving the glycoside conversion rate. Therefore, we successfully established a dual pathway for the synergistic synthesis of hypoxanthine using AMP and IMP without adenylate accumulation.

In conjunction with de novo nucleotide synthesis from simple precursors, organisms use a complementary

purine base pathway regulated by purine salvage genes [33]. The corresponding nucleotides were synthesized from PRPP and various purines [2, 34]. Hypoxanthine phosphoribosyltransferase (i.e., encoded by the *hpt* gene) converts hypoxanthine in the purine nucleoside pool into IMP [35]. As the path of least resistance in the context of expended metabolic energy, since the remedial pathway consumes less energy than the 'de novo synthesis' pathway, this makes it the optimal pathway for nucleotide synthesis (i.e., when bases or nucleosides are readily available in the surrounding environment). Therefore, we hypothesized that knocking out hypoxanthine phosphoribosyltransferase (encoded by the *hpt* gene) could increase the accumulation of hypoxanthine. To test this hypothesis we created strain Y4-3 by knocking out *hpt* in the Y4-2 strain. After 24 h of shake-flask fermentation (Fig. 3F), hypoxanthine titer in Y4-3 reached 2.89 g/L, with a conversion rate of 0.06 g / g, 23.4% (i.e., higher than that of the control strain Y4-2). However, the resultant biomass did not change significantly, an outcome congruent with outcomes of previous studies.

Dynamic regulation of *guaB* to weaken the xanthine and guanine branch pathways

IMP is a key metabolic node in purine synthesis. Previous studies showed guanine and xanthine accumulation, highlighting the need to study the branch of IMP in the direction of these compounds. In this study, the *guaB* gene was knocked out in the Y4-3 strain, creating strain Y5-1. Shake-flask fermentation results, as shown in Fig. 4, revealed that the OD600 value of Y5-1 decreased to 34, and the hypoxanthine titer decreased to 2.11 g/L, with no accumulation of guanine and xanthine. This indicates that blocking the guanine and xanthine branches severely affects bacterial growth and production. When 0.3 g/L guanosine was added to the medium, hypoxanthine production in the Y5-1 strain increased to 3.43 g/L, and the OD600 value rose to 47, indicating a significant recovery in OD600 and hypoxanthine production.

Static knockout of the *guaB* gene, though beneficial for hypoxanthine production, results in undesirable auxotrophic strains. Therefore, to balance growth and product synthesis, we dynamically regulated the expression of the *guaB* gene, providing endogenous guanine and xanthine to construct non-nutritive strains. During the transition of *E. coli* from the exponential growth phase to the stationary phase, *guaB* expression decreased, indicating a shift from growth to production mode.

CRISPR interference (CRISPRi) and inducible promoters are effective tools for dynamic metabolic flux regulation in bacteria [36]. However, CRISPRi systems require thermal or chemical inducers that complicate the production process and are costly, which is unsuitable for large-scale industrial production. The Quorum-Sensing

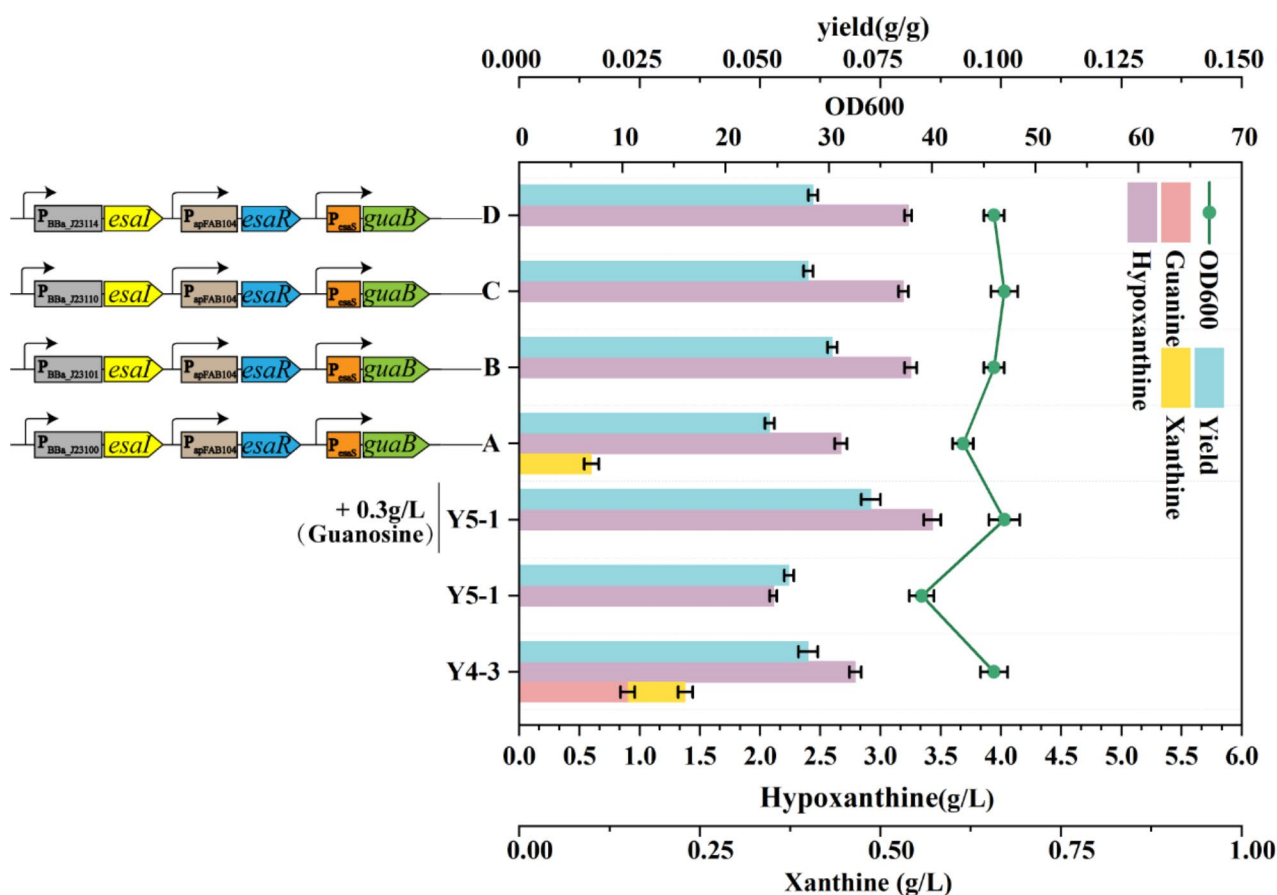


Fig. 4 Effects of deleting the *guaB* gene and replacing the *esaI* promoter with different intensities in the Quorum-Sensing circuit system on the strain. Data are expressed as means, and the error bars represent the standard deviation ($n=3$ independent experiments)

circuit (*Esa* QS system) dynamic dial switch from *Pan-tocaea stewartii* [37] is advantageous for strain modification. QS systems respond to cell density and control gene expression and have been applied in *E. coli*, *S. cerevisiae*, and other biosynthetic products [38–40]. Therefore, we introduced a QS system to regulate *guaB* expression. As shown in Fig. 4, *guaB* expression is controlled by the P_{esaS} promoter, activated by the transcriptional regulator *EsaR* in the absence of acyl homoserine lactone (AHL) signaling molecules. When AHL accumulates, the P_{esaS} promoter is inactivated, halting *guaB* transcription. The *EsaI* gene, which controls AHL production, is essential for triggering system switching. The *EsaR* gene, controlled by the P_{apFAB104} promoter, was introduced into Y5-1 to create strain Y5-2, and the natural *guaB* promoter was replaced with P_{esaS} to obtain strain Y5-3. The *EsaI* gene, under the control of different intensity promoters, was introduced into the *ygaY* locus of the Y5-4 strain. $P_{\text{BBa}_j23114} < P_{\text{BBa}_j23110} < P_{\text{BBa}_j23101} < P_{\text{BBa}_j23100}$ (The specific sequence is shown in Supplementary Table 2) formed A, B, C, and D strains. Compared to control strain Y5-1, the cell growth in strains A, B, C, and D

increased significantly. The hypoxanthine titer of strain A reached 2.67 g/L, and OD600 was 43, producing 0.1 g/L of xanthine. The hypoxanthine titer of strain B reached 3.25 g/L, with an OD600 of 46. The hypoxanthine titer of strain C reached 3.19 g/L, with an OD600 of 45. The hypoxanthine titer of strain D reached 3.23 g/L, with an OD600 of 47. Strain A still accumulated a small amount of xanthine, indicating that the *EsaI* gene under the control of this strong promoter was weak and insufficient to regulate the *guaB* gene. After adding the strain B promoter, the hypoxanthine titer and biomass decreased slightly, indicating excessive promoter strength, which hindered bacterial growth. We concluded that strain Y5-4B exhibited the highest hypoxanthine titer.

Precursor strengthening

During the construction of the chassis strains, we over-expressed the purine operon from *B. subtilis*. It has been reported that the metabolic flow of PRPP to the purine pathway is 30–40% of the total flow [41]. However, there is still potential for further optimization. Therefore, we integrated the operon again and obtained strain Y6 based

on strain Y5-4B. After 24 h of shake-flask fermentation, strain Y6 showed (Fig. 5A) no significant increase in hypoxanthine titer, with biomass remaining unaffected. The purine operon requires glutamine, glycine, and aspartic acid as precursors in the synthesis of IMP, with PRPP as a precursor. We hypothesized that the lack of precursors limits the reaction; therefore, we set up eight control groups and performed shake-flask fermentation for 24 h. As shown in Fig. 5B, the hypoxanthine titers of the control groups with glutamine, aspartic acid, and a combination of both increased to varying degrees. However, glycine addition did not significantly change the titers, indicating that the glycine synthesized by the bacteria was sufficient for the reaction. These results verified our hypothesis that insufficient glutamine and aspartic acid synthesis limited the purine operon reaction. Therefore, we further explored how to enhance the synthesis of the precursors, namely, glutamine and aspartic acid. L-glutamic acid and ammonia are combined

with glutamine synthetase (encoded by *glnA*) to produce glutamine(L-gln). In *E. coli*, glutamine synthetase activity is inhibited by various metabolites [42] and is sensitive to the concentration of ammonium ions (NH_4^+). High NH_4^+ levels in *E. coli* lead to *glnA* adenylation, resulting in loss of activity [43]. However, because the homologous enzyme from Gram-positive bacteria is not sensitive to NH_4^+ , we introduced the *glnA*_{bsu}^{L159I.E304A} mutant from *B. subtilis* [44, 45], creating strain Y6-1. After 24 h of shake-flask fermentation, the hypoxanthine titer reached 3.61 g/L, an 11% increase. The introduction of *glnA*_{bsu}^{L159I.E304A} mutant, promoted the conversion of L-glutamic acid to L-gln in the cells, improved glutamine availability in the bacteria, and contributed to the synthesis of hypoxanthine.

Oxaloacetic acid and glutamic acid are catalyzed by aspartate aminotransferase (encoded by *aspC*) to generate aspartic acid. To enhance aspartic acid synthesis, we overexpressed the aspartic acid transaminase P_{trc}-*aspC*

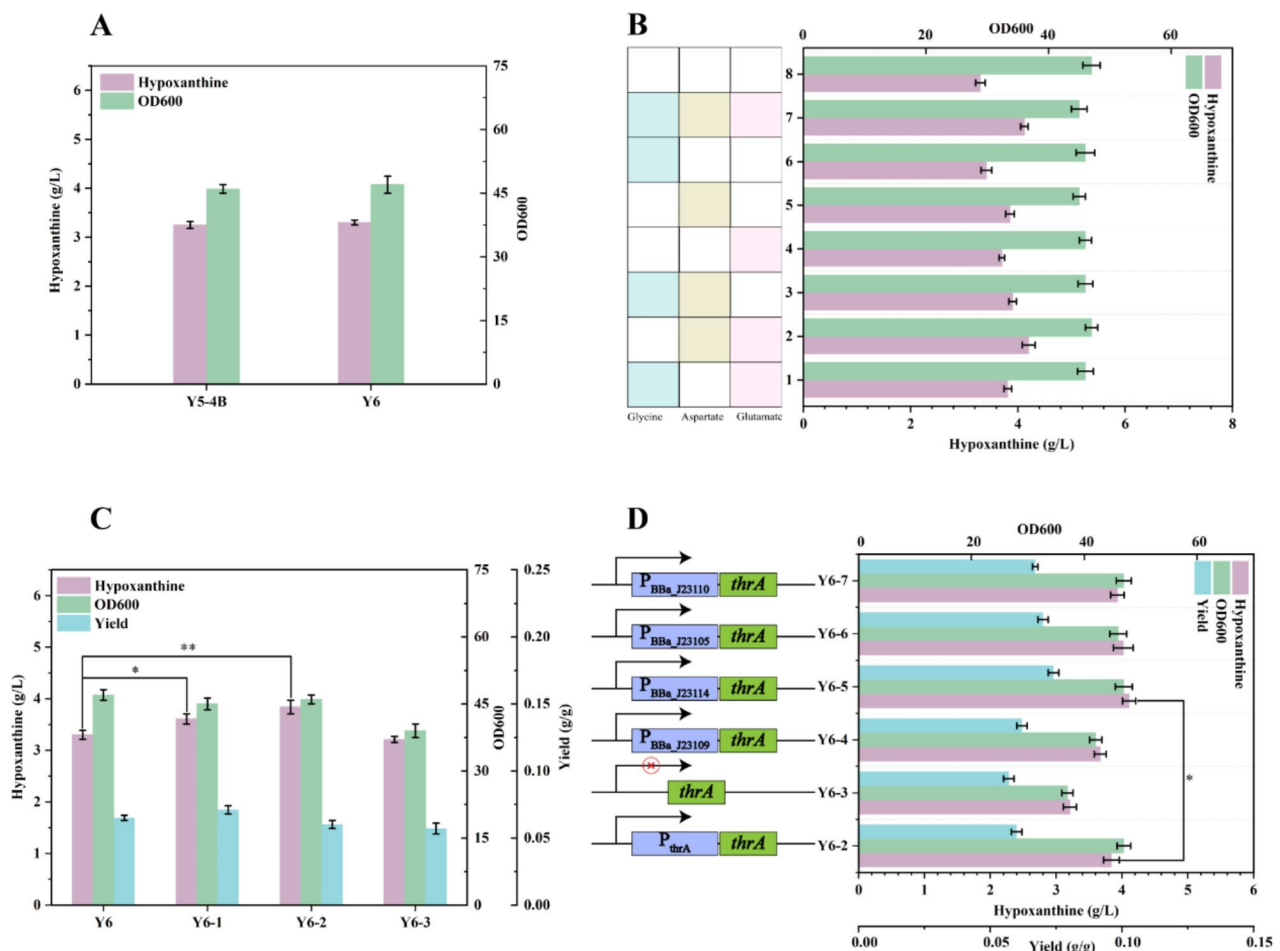


Fig. 5 (A) Molecular structure diagram of hypoxanthine. (B) Effects of adding glycine, aspartic acid, and glutamine on the strain. (C) Effects of overexpressing glutamine synthetase, aspartate aminotransferase, and knocking out bifunctional aspartokinase on bacterial strains. (D) Effect of deleting or integrating bifunctional aspartokinase with different strength promoters on the strain. Data are expressed as means, and the error bars represent the standard deviation ($n=3$ independent experiments)

at the genomic level, resulting in strain Y6-2 from Y6-1. After verification, the titer of strain Y6-2 was 3.84 g/L. Although the titer improved, the glycoside conversion rate decreased from 0.071 g/g to 0.06 g/g. This may be because excessive aspartic acid flows into the synthesis pathway of branched amino acids. To address this, we knocked out bifunctional aspartokinase (encoded by *thrA*), which encodes the main branch of aspartic acid, to reduce its conversion to other amino acids. Strain Y6-3 was obtained, and after 24 h of shake-flask fermentation, the hypoxanthine titer was 3.21 g/L, with an OD600 of 39. These results indicated that the growth and titer of the strain were affected, indicating that directly blocking the branch was not feasible. Therefore, we used promoter engineering to weaken the pathway. We replaced the *thrA* gene promoter with promoters of varying strength (from weak to strong: j23109 < J23114 < j23105 < J23110). The specific sequence is shown in Supplementary Table 2. The outcomes of shake-flask fermentation confirmed the normalization for the growth of the strain integrated with the J23114 promoter. The hypoxanthine titer reached 4.11 g/L, with a conversion rate of 0.074 g/g. These were the highest titer and conversion rates, indicating that proper regulation of promoter strength in the aspartic branch pathway improves product synthesis and conversion rate. We named this high-yielding hypoxanthine strain YZ.

Fed-batch fermentation in a 5-L bioreactor

Fed-batch fermentation was carried out in a 5 L bioreactor to evaluate the potential production performance of the engineered strain YZ. The fermentation tank temperature is maintained at 37 °C, with the pH kept around 6.7 throughout the process. By increasing the rotational speed, the dissolved oxygen concentration is sustained, creating optimal conditions for strain growth and production. As shown in Fig. 6, an initial glucose concentration of 20 g/L is provided at the start of fermentation.

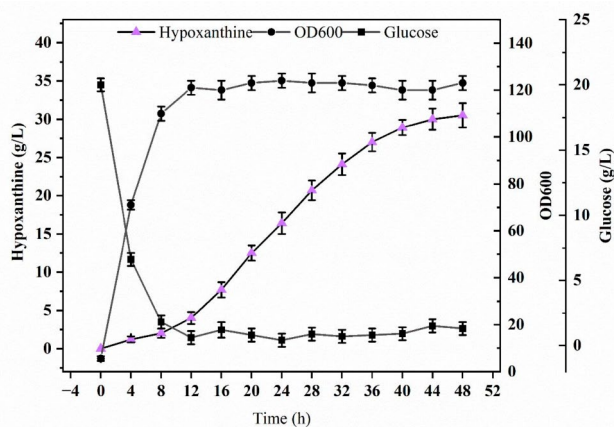


Fig. 6 A. Fermentation data of the YZ strain in a 5L fermentor

After 8 h, when glucose levels near depletion, a controlled supplementation rate is applied to keep the residual glucose concentration below 2 g/L. The results showed that the logarithmic growth of the cells continued until 12 h of fermentation and then gradually entered a stable period, with biomass peaking at 12 h (Fig. 6). The hypoxanthine titer increased exponentially after 12 h of fermentation, with the growth rate declining after 32 h and reaching a maximum concentration of 30.6 g/L at 48 h. Acid production intensity peaked at 1.4 g/L/h in the 12–32 h interval. To the best of our knowledge, these values represent the highest reported titers and efficiencies for hypoxanthine production from glucose. Additionally, liquid-phase test results indicated minimal by-product generation, facilitating the implementation of downstream processing.

Discussion

First, based on previous studies, we knocked out the decomposition pathway of hypoxanthine and the repressor protein PurR and explored the effects of various *purF* and *prs* point mutations to relieve feedback inhibition. The optimal mutants identified were *purF*_{bsu}^{D293V, K316Q, S400W} and *prs*_{eco}^{D128A}. To enhance the metabolic flow of the key precursor, PRPP, *pur* (*FDNTSQLMKECB*), a purine operon from *B. subtilis*, was introduced to obtain the chassis strain HY5. In previous studies, the method of directly blocking the branch pathway was often adopted to increase metabolic flow to the target product. Therefore, we attempted to knock out the adenine branches. Although this method improved the titer slightly, it also caused strain defects.

Strain defects affect bacterial growth and limit titer increase. However, adding defects to the fermentation process is necessary, as it significantly increases production costs and may complicate downstream extraction. Therefore, to avoid the production of auxotrophic strains, we introduced the *purA*_{bsu}^{P242N} mutant gene with weaker enzyme activity. Experimental results showed that, although this approach was better than direct knockout, biomass and titer increased only with the addition of adenosine. Although this method was effective, its outputs were sufficient through the lens of the primary objectives of this study. By knocking out adenosine deaminase and adenine deaminase, we observed a reduction in hypoxanthine titer, confirming that part of the metabolic flow in the previous hypoxanthine synthesis was derived from the adenine synthesis pathway. Therefore, we constructed a dual pathway for the synergistic synthesis of hypoxanthine using AMP and IMP. After experimental comparisons, it was found that *E. coli*'s adenosine deaminase gene *add* and adenine deaminase gene *ade* had a synergistic effect, significantly promoting hypoxanthine synthesis and improving the conversion rate. In addition, due to feedback inhibition of adenylate in the purine

synthesis pathway, the accumulation of adenylyate cannot be ignored. We introduced IMP-specific 5'-nucleotidase from *S. cerevisiae*, diverting more metabolic flux to the hypoxanthine synthesis pathway to address adenylyate accumulation. Then, we blocked the backup reaction of hypoxanthine to generate inosinic acid, which significantly improved the titer and conversion rate. We then dynamically regulated the *guaB* gene, using the Esa QS system from *Pantoea stewartii*, achieving endogenous guanine and xanthine supply. Since the metabolic flux of the purine synthesis pathway accounts for approximately 30–40% of the total PRPP, which is only a small part, we used three copies of the *pur* (*FDNTSQLMKECB*) operon to further increase the titer. The results showed that the increase in titer was not significant.

Further experiments verified that insufficient synthesis of glutamine and aspartic acid limited the titer increase; therefore, a glutamine synthetase mutant was introduced to enhance glutamine synthesis. In addition, overexpression of the aspartate aminotransferase *aspC* gene increased the titer but decreased the glycoside conversion rate, likely due to aspartic acid synthesis flowing to its branched amino acid pathway. To address this, we weakened the promoter of the *thrA* gene encoding the main aspartate kinase, ultimately increasing the hypoxanthine titer and glycoside conversion rate. After 48 h of fed-batch fermentation, the final titer reached 30.6 g/L, with the highest rate at 1.4 g/L/h. Thus, we successfully constructed a hypoxanthine-engineered strain with the highest reported titer.

While we have developed a high-yield strain for hypoxanthine production, the glycoside conversion rate remains relatively low, leaving considerable room for improvement. The current strain modification did not target the central carbon metabolism pathway. Optimizing this pathway could significantly enhance precursor utilization efficiency [46–48]. This approach would enhance the conversion rate and overall strain performance. Our subsequent experiments will focus on redirecting more carbon metabolism towards the pentose phosphate pathway (PPP).

Conclusions

A plasmid-free, non-induced, non-defective, high-yield hypoxanthine strain was engineered using *E. coli* as the chassis strain. The modifications included (1) blocking the hypoxanthine degradation pathway and removing transcriptional repression and feedback inhibition in the purine synthesis pathway; (2) introducing exogenous adenosine deaminase and adenine deaminase to create a dual pathway for hypoxanthine synthesis from AMP and IMP. We also introduced an IMP-specific 5'-nucleotidase to address the issue of adenylyate accumulation; (3) dynamically regulating the *guaB* gene; and (4) regulating the

supply of precursor molecules glutamine and L-aspartic acid. After 48 h of fed-batch fermentation, the engineered strain achieved a hypoxanthine titer of 30.6 g/L, with a yield of 0.071 g/g glucose and a maximum production rate of 1.4 g/L/h. These metrics represent the highest titer, yield, and production rate of hypoxanthine reported in the context of microbial fermentation, laying a foundation for the application of this method in an industrial scale.

Abbreviations

IMP	Inosine 5'-monophosphate
AMP	Adenosine 5'-monophosphate
PCR	Polymerase chain reaction
GMP	Guanosine 5'-phosphate
CRISPRi	CRISPR interference
QS	Quorum-Sensing
NH ⁴⁺	Ammonium ions
AHL	Acyl homoserine lactone

Supplementary Information

The online version contains supplementary material available at <https://doi.org/10.1186/s12934-024-02576-x>.

Supplementary Material 1

Acknowledgements

The supply of yeast extract and peptone for the research is gratefully acknowledged to Lesaffre.

Author contributions

SYZ: Investigation, Visualization, Writing - Original Draft. TES: Methodology, Visualization. LWL, ZCC, CGL, ZCY, PJS: Visualization. QYX: Conceptualization, writing—review and editing, supervision.

Funding

This study was supported by the Shandong Province Key R&D Plan Project (grant number 2021ZDSYS10).

Data availability

No datasets were generated or analysed during the current study.

Declarations

Ethics approval and consent to participate

Not applicable.

Consent for publication

Not applicable.

Competing interests

The authors declare no competing interests.

Received: 3 July 2024 / Accepted: 2 November 2024

Published online: 14 November 2024

References

1. Maiuolo J, Oppedisano F, Gratteri S, Muscoli C, Mollace V. Regulation of uric acid metabolism and excretion. *Int J Cardiol*. 2016;213:8–14.
2. Pedley AM, Benkovic SJ. A New View into the regulation of Purine Metabolism: the purinosome. *Trends Biochem Sci*. 2017;42:141–54.
3. Cohen S, Jordheim LP, Megherbi M, Dumontet C, Guittou J. Liquid chromatographic methods for the determination of endogenous nucleotides and

- nucleotide analogs used in cancer therapy: a review. *J Chromatogr B Analyt Technol Biomed Life Sci.* 2010;878:1912–28.
4. Shi T, Wang Y, Wang Z, Wang G, Liu D, Fu J, et al. Deregulation of purine pathway in *Bacillus subtilis* and its use in riboflavin biosynthesis. *Microb Cell Fact.* 2014;13:101.
 5. Ledesma-Amaro R, Buey RM, Revuelta JL. Increased production of inosine and guanosine by means of metabolic engineering of the purine pathway in *Ashbya Gossypii*. *Microb Cell Fact.* 2015;14:58.
 6. Matsui H, Kawasaki H, Shimaoka M, Kurahashi O. Investigation of various genotype characteristics for inosine accumulation in *Escherichia coli* W3110. *Biosci Biotechnol Biochem.* 2001;65:570–8.
 7. Liu M, Fu Y, Gao W, Xian M, Zhao G. Highly efficient biosynthesis of Hypoxanthine in *Escherichia coli* and Transcriptome-based analysis of the Purine metabolism. *ACS Synth Biol.* 2020;9:525–35.
 8. Cordell RL, Hill SJ, Ortori CA, Barrett DA. Quantitative profiling of nucleotides and related phosphate-containing metabolites in cultured mammalian cells by liquid chromatography tandem electrospray mass spectrometry. *J Chromatogr B Analyt Technol Biomed Life Sci.* 2008;871:115–24.
 9. Traut TW. Physiological concentrations of purines and pyrimidines. *Mol Cell Biochem.* 1994;140:1–22.
 10. Guimarães PMR, Londesborough J. The adenylate energy charge and specific fermentation rate of brewer's yeasts fermenting high- and very high-gravity worts. *Yeast.* 2008;25:47–58.
 11. Shimaoka M, Takenaka Y, Kurahashi O, Kawasaki H, Matsui H. Effect of amplification of desensitized *purF* and *prs* on inosine accumulation in *Escherichia coli*. *J Biosci Bioeng.* 2007;103:255–61.
 12. He B, Shiao A, Choi KY, Zalkin H, Smith JM. Genes of the *Escherichia coli* *pur* regulon are negatively controlled by a repressor-operator interaction. *J Bacteriol.* 1990;172:4555–62.
 13. Meng LM, Nygaard P. Identification of hypoxanthine and guanine as the co-repressors for the purine regulon genes of *Escherichia coli*. *Mol Microbiol.* 1990;4:2187–92.
 14. Li Y, Lin Z, Huang C, Zhang Y, Wang Z, Tang Y-J, et al. Metabolic engineering of *Escherichia coli* using CRISPR-Cas9 mediated genome editing. *Metab Eng.* 2015;31:13–21.
 15. Wu H, Li Y, Ma Q, Li Q, Jia Z, Yang B, et al. Metabolic engineering of *Escherichia coli* for high-yield uridine production. *Metab Eng.* 2018;49:248–56.
 16. Lobanov KV, korol'kova NV, Eremina SI, Érrais Lopes L, Mironov AS. [Mutation analysis of the purine operon leader region in *Bacillus subtilis*]. *Genetika.* 2011;47:890–9.
 17. Huffman JL, Lu F, Zalkin H, Brennan RG. Role of residue 147 in the gene regulatory function of the *Escherichia coli* purine repressor. *Biochemistry.* 2002;41:5111–20.
 18. Zakataeva NP, Romanenkov DV, Skripnikova VS, Vitushkina MV, Livshits VA, Kivero AD, et al. Wild-type and feedback-resistant phosphoribosyl pyrophosphate synthetases from *Bacillus amyloliquefaciens*: purification, characterization, and application to increase purine nucleoside production. *Appl Microbiol Biotechnol.* 2012;93:2023–33.
 19. Ebbole DJ, Zalkin H. *Bacillus subtilis* *pur* operon expression and regulation. *J Bacteriol.* 1989;171:2136–41.
 20. Ebbole DJ, Zalkin H. Cloning and characterization of a 12-gene cluster from *Bacillus subtilis* encoding nine enzymes for de novo purine nucleotide synthesis. *J Biol Chem.* 1987;262:8274–87.
 21. Li H, Zhang G, Deng A, Chen N, Wen T. De novo engineering and metabolic flux analysis of inosine biosynthesis in *Bacillus subtilis*. *Biotechnol Lett.* 2011;33:1575–80.
 22. Wang X, Wang G, Li X, Fu J, Chen T, Wang Z, et al. Directed evolution of adenylosuccinate synthetase from *Bacillus subtilis* and its application in metabolic engineering. *J Biotechnol.* 2016;231:115–21.
 23. Chang ZY, Nygaard P, Chinault AC, Kellems RE. Deduced amino acid sequence of *Escherichia coli* adenosine deaminase reveals evolutionarily conserved amino acid residues: implications for catalytic function. *Biochemistry.* 1991;30:2273–80.
 24. Akesson AL, Wiginton DA, Dusing MR, States JC, Hutton JJ. Mutant human adenosine deaminase alleles and their expression by transfection into fibroblasts. *J Biol Chem.* 1988;263:16291–6.
 25. Lupidi G, Marmocchi F, Falasca M, Venardi G, Cristalli G, Grifantini M, et al. Adenosine deaminase from *Saccharomyces cerevisiae*: kinetics and interaction with transition and ground state inhibitors. *Biochim Biophys Acta.* 1992;1122:311–6.
 26. Nygaard P, Duckert P, Saxild HH. Role of adenosine deaminase in purine salvage and nitrogen metabolism and characterization of the *ade* gene in *Bacillus subtilis*. *J Bacteriol.* 1996;178:846–53.
 27. Matsui H, Shimaoka M, Kawasaki H, Takenaka Y, Kurahashi O. Adenosine deaminase activity of the *yicP* gene product of *Escherichia coli*. *Biosci Biotechnol Biochem.* 2001;65:1112–8.
 28. Rouf MA, Lompfrey RF. Degradation of uric acid by certain aerobic bacteria. *J Bacteriol.* 1968;96:617–22.
 29. Deeley MC. Adenosine deaminase and adenosine utilization in *Saccharomyces cerevisiae*. *J Bacteriol.* 1992;174:3102–10.
 30. Shimaoka M, Kawasaki H, Takenaka Y, Kurahashi O, Matsui H. Effects of *Edd* and *pgi* disruptions on inosine accumulation in *Escherichia coli*. *Biosci Biotechnol Biochem.* 2005;69:1248–55.
 31. Ebbole DJ, Zalkin H. Interaction of a putative repressor protein with an extended control region of the *Bacillus subtilis* *pur* operon. *J Biol Chem.* 1989;264:3553–61.
 32. Itoh R, Saint-Marc C, Chaignepain S, Katakura R, Schmitter J-M, Daignan-Fornier B. The yeast *ISN1* (*YOR155c*) gene encodes a new type of IMP-specific 5'-nucleotidase. *BMC Biochem.* 2003;4:4.
 33. Ding H, Yue L-J, Yang C-L. [Research progress in hypoxanthine-guanine phosphoribosyltransferase]. *Yi Chuan.* 2013;35:948–54.
 34. Kappock TJ, Ealick SE, Stubbe J. Modular evolution of the purine biosynthetic pathway. *Curr Opin Chem Biol.* 2000;4:567–72.
 35. Ljungdahl PO, Daignan-Fornier B. Regulation of amino acid, nucleotide, and phosphate metabolism in *Saccharomyces cerevisiae*. *Genetics.* 2012;190:885–929.
 36. Zhang C, Li Y, Ma J, Liu Y, He J, Li Y, et al. High production of 4-hydroxyisoleucine in *Corynebacterium glutamicum* by multistep metabolic engineering. *Metab Eng.* 2018;49:287–98.
 37. Shong J, Collins CH. Engineering the *esaR* promoter for tunable quorum sensing-dependent gene expression. *ACS Synth Biol.* 2013;3:568–75.
 38. Pai A, Tanouchi Y, You L. Optimality and robustness in quorum sensing (QS)-mediated regulation of a costly public good enzyme. *Proc Natl Acad Sci U S A.* 2012;109:19810–5.
 39. Shen Y-P, Fong LS, Yan Z-B, Liu J-Z. Combining directed evolution of pathway enzymes and dynamic pathway regulation using a quorum-sensing circuit to improve the production of 4-hydroxyphenylacetic acid in *Escherichia coli*. *Biotechnol Biofuels.* 2019;12:94.
 40. Williams TC, Aversch NJH, Winter G, Plan MR, Vickers CE, Nielsen LK, et al. Quorum-sensing linked RNA interference for dynamic metabolic pathway control in *Saccharomyces cerevisiae*. *Metab Eng.* 2015;29:124–34.
 41. Jensen KF, Dandanell G, Hove-Jensen B, Willemoës M. Nucleotides, nucleosides, and Nucleobases. *EcoSal Plus.* 2008;3.
 42. Stadtman ER. Regulation of glutamine synthetase activity. *EcoSal Plus.* 2004;1.
 43. Mangum JH, Magni G, Stadtman ER. Regulation of glutamine synthetase adenylation and deadenylation by the enzymatic uridylation and deadenylation of the PII regulatory protein. *Arch Biochem Biophys.* 1973;158:514–25.
 44. Wray LV, Fisher SH. Functional roles of the conserved Glu304 loop of *Bacillus subtilis* glutamine synthetase. *J Bacteriol.* 2010;192:5018–25.
 45. Li Z, Ding D, Wang H, Liu L, Fang H, Chen T, et al. Engineering *Escherichia coli* to improve tryptophan production via genetic manipulation of precursor and cofactor pathways. *Synth Syst Biotechnol.* 2020;5:200–5.
 46. Deng A, Qiu Q, Sun Q, Chen Z, Wang J, Zhang Y, et al. In silico-guided metabolic engineering of *Bacillus subtilis* for efficient biosynthesis of purine nucleosides by blocking the key backflow nodes. *Biotechnol Biofuels Bio-prod.* 2022;15:82.
 47. Li B, Zhang B, Wang P, Cai X, Chen Y-Y, Yang Y-F, et al. Rerouting fluxes of the Central Carbon Metabolism and relieving mechanism-based inactivation of L-Aspartate- α -decarboxylase for fermentative production of β -Alanine in *Escherichia coli*. *ACS Synth Biol.* 2022;11:1908–18.
 48. Wu H, Tian D, Fan X, Fan W, Zhang Y, Jiang S, et al. Highly efficient production of L-Histidine from glucose by metabolically engineered *Escherichia coli*. *ACS Synth Biol.* 2020;9:1813–22.

Publisher's note

Springer Nature remains neutral with regard to jurisdictional claims in published maps and institutional affiliations.